Journal of Materials Research and Technology 38 (2025) 1724–1733

Contents lists available at ScienceDirect

Journal of Materials Research and Technology

journal homepage: www.elsevier.com/locate/jmrt

Effect of 3D printing settings on the mechanical properties and biocompatibility of polymeric materials used for 3D direct printing of orthodontic aligners

Marco Migliorati [a], Sara Drago [a,d,*], Martina Lenzuni [b], Alessandra Marrella [b], Paolo Giannoni [c], Alberto Lagazzo [d]

[a] Department of Integrated Diagnostic and Surgical Sciences, University of Genoa, Genoa, Italy
[b] Institute of Electronics, Computer and Telecommunication Engineering (IEIIT), National Research Council of Italy (CNR), Genoa, Italy
[c] Department of Experimental Medicine, Biology Section, University of Genoa, Genoa, Italy
[d] Department of Civil, Chemical and Environmental Engineering, University of Genoa, Genoa, Italy

ARTICLE INFO

Handling editor: P.Y. Chen

Keywords:
3D printing
Additive manufacturing
Biocompatible resin
Dental materials
Vat-polymerization

ABSTRACT

The advent of the biocompatible resin Tera Harz TC-85 DAC (TC-85) introduces the potential for direct 3D-printed aligners via vat-polymerization, where photosensitive liquids are hardened layer by layer using a light source. This study investigates the influence of tunable printing parameters on the mechanical and biocompatibility properties of the resulting materials. Specimens were fabricated using two different printers with varying Z resolutions (50 μm and 100 μm), output thicknesses (2 mm, 1 mm, and 0.5 mm), and feeding resins (TC-85 and Clear A). Mechanical properties were evaluated through tensile and bending tests, and the results demonstrate that printer selection significantly affects mechanical properties such as ductility and rigidity. In contrast, variations in Z resolution did not exhibit a significant impact. Material choice was identified as a critical factor, significantly influencing the elastic modulus (1131 vs 2088 MPa for TC-85 and Clear A resins, respectively), ultimate tensile strength (23 vs 41 MPa), and elongation at break (66 % vs 16 %), thereby affecting the overall mechanical behavior of the samples. Biological assays did not evidence impairment of cell viability or proliferative capacities for the used cell lines in any applied experimental condition. Overall, this study underscores the role of printer type and material selection in optimizing the performance of direct 3D-printed aligners, highlighting key factors for future advancements in the field of dental materials and additive manufacturing technologies.

1. Introduction

Traditional fixed orthodontic appliances consist of brackets that are bonded individually to each tooth. Each bracket features a central slot intended to hold an archwire, which exerts the correct force to move the teeth. This system dates back to the Angle technique and materials developed in the early 1900s, utilizing standard brackets that were identical for all teeth and featured a slot perpendicular to the bracket base [1]. Since these brackets were not anatomically tailored to each tooth, the orthodontist had to manually shape the archwire by creating specific bends to control labial/buccal, mesio-distal, and vestibulo-lingual inclinations. Andrews' introduction of an individualized prescription for each bracket, designed to precisely specify the desired tip and torque of that tooth, aimed to both simplify and improve the efficiency of tooth movement and enhance clinical management for the orthodontist, who was relieved from the task of applying a large number of bends on the wires [2]. This technique, which is known as multibracket appliance, is a powerful biomechanical tool to solve even complex malocclusions, for both the adult and the adolescent patient; its usage before the completion of dental permutation is somewhat limited, and it is not indicated in case of dental allergies [3].

Dental aligners have revolutionized orthodontic treatment in recent years, offering a more discreet and comfortable alternative to traditional metal braces, capable of overcoming some of the previously described issues. These aligners are typically fabricated using transparent thermoplastic resins and, increasingly, through 3D printing technologies,

* Corresponding author. Largo R. Benzi 10, 16100, Genova, Italy.
E-mail address: sara.drago@edu.unige.it (S. Drago).

https://doi.org/10.1016/j.jmrt.2025.07.247
Received 14 January 2025; Received in revised form 23 July 2025; Accepted 27 July 2025
Available online 29 July 2025

which must meet specific requirements for mechanical performance, biocompatibility, and aesthetic appeal [4]. Several 3D-printable resins have been introduced for dental purposes, such as BioMed Amber, IBT and Dental LT Clear, which marked an important step toward custom in-office production [5,6]. In this context, the introduction of the novel biocompatible resin Tera Harz TC-85 DAC (shortly called TC-85), developed by Graphy Inc. (Seoul, Republic of Korea), represents a further innovation. This resin, a known CE (Conformité Européenne) Class-IIa material, has received approval from both the Korean and United States FDA for clear aligner direct 3D printing [7]. What distinguishes TC-85 from earlier resins is its reported shape memory behavior, which potentially reduces the number of aligners required during treatment [8]. In addition, Clear A resin has emerged as another promising material for clear aligner fabrication. Similar to TC-85, Clear A has been recently used in the production of polyurethane-based aligners, offering an alternative for effective orthodontic treatment [9].

The fabrication of dental aligners involves advanced manufacturing technologies, with 3D printing being one of the most commonly used methods, particularly with vat-polymerization procedures. Additive manufacturing offers significant advantages in terms of precision, customization, and speed, enabling the production of aligners tailored to the individual patient's anatomy. Major techniques are stereolithography (SLA), digital light processing (DLP), and liquid crystal display (LCD), distinguished by the respective UV sources: a laser beam, a digital projector, and an LCD screen [10–12]. In recent years, growing attention has been devoted to the 3D printing of advanced polymers and ceramics for biomedical applications, including orthodontics, due to their tunable mechanical and biological properties [13,14]. These developments highlight the broader relevance and versatility of additive manufacturing technologies across multiple materials. Several studies have proved the accuracy of these printing strategies in aligner production, although entry-level LCD technologies have exhibited greater deviations in accuracy compared to others [15–17].

The choice of resin, printing resolution, and sample thickness are among the factors that mostly impact the mechanical and functional properties of the printed aligners. Understanding how these variables influence the aligner's performance is crucial for optimizing the material properties and achieving the desired clinical outcomes. For example, Zinelis et al. [18] recently compared the mechanical properties of orthodontic aligners produced by five commercially available 3D printers using TC-85 as the resin, with significant differences observed across the printers in the mechanical properties. In particular, aligners from LCD printers showed superior mechanical properties compared to those from DLP printers.

Each 3D printer is characterized by specific resolutions along the XY plane (horizontal) and the Z axis (vertical), which are both crucial for achieving dimensional accuracy in printed objects. The XY resolution refers to the smallest movement the printer can make in the horizontal plane and is typically determined by the precision of the light source used (e.g., UV light in resin printers) [19]. The Z resolution, on the other hand, corresponds to the minimum layer height the printer can produce vertically, directly affecting the surface smoothness and detail along the vertical axis. This parameter can often be adjusted depending on the material and printer, with common layer thicknesses being 25 μm, 50 μm, and 100 μm [10,12]. It has to be noted that a higher resolution does not necessarily coincide with increased accuracy: it requires longer printing sessions and a greater number of layers, which in turn enhances the risk of errors or failure [10].

The performance of different resins under varying conditions (differences in printing resolutions, sample thickness, specific 3D technology applied, etc.) has been -so far- poorly investigated. It is essential to assess how these factors affect the mechanical behavior of the printed materials, particularly their tensile strength, bending resistance, and overall structural integrity. In addition to mechanical properties, biocompatibility is a vital parameter in the selection of materials for medical applications [20,21]. Dental aligners are indeed in direct contact with the oral mucosa for extended periods, raising needs for rigorous testing for cytotoxicity and cellular responses. The interaction of the resins with human cells is indeed critical to their safety and effectiveness: for example, it has been reported that the release of potentially harmful substances, such as bisphenol A (BPA), from 3D printed aligners can lead to adverse effects, including cytotoxicity and genotoxicity [22]. Given the increasing use of these materials in orthodontics, it is essential to conduct comprehensive biocompatibility and mechanical assessments to ensure that these devices do not pose risks to patients.

In this respect, the primary aim of this study was to compare the mechanical properties of TC-85 and Clear A resins, considering different 3D printing resolutions, sample thicknesses, and printing technologies. By conducting tensile and bending tests, the strength, flexibility, and resilience of samples were assessed. This study uniquely evaluates the interplay between resin type, printing resolution, and sample thickness to optimize aligner performance—a crucial aspect overlooked in prior studies. Furthermore, cell proliferation and cell adhesion assays were performed on two cell lines to evaluate the biological safety of the proposed material. Such a comprehensive comparison can help identify the resin and printing set up parameters that offer the best combination of mechanical performance, printability, and biocompatibility, thus providing valuable guidance for the selection of materials in the fabrication of dental aligners.

2. Materials & methods

2.1. Materials

Two photopolymer resins were utilized for sample production: Tera Harz TC-85 DAC resin (TC-85, Graphy Inc., Seoul, Korea) and Clear A resin (Senertek, Karatas, Izmir, Turkey). Phosphate buffered saline (PBS) was purchased from VWR (Leuven, Belgium). F12-medium was purchased from Biochrom AG (Berlin, Germany) and Dulbecco's modified Eagle's Medium (DMEM, high glucose) from EuroClone S.p.A. (Milan, Italy). Invitrogen Presto Blue™ Cell Viability Reagent (cat. n. A13262) was purchased from ThermoFisher (Monza, Italy).

2.2. Sample design and fabrication

Samples were designed using UltiMaker Cura CAD modeling software based on STL files. Two geometries were employed, tailored to the specific mechanical tests to be performed: dog-bone and parallelepiped shapes. The dog-bone samples were designed with an overall width of 20 mm, a gauge width of 10 mm, an overall length of 90 mm, and thicknesses of 2 mm, 1 mm, or 0.5 mm, depending on the experimental group (Fig. 1 (a)). The parallelepiped samples were designed with a width of 12 mm, a length of 80.5 mm, and thicknesses of 2 mm or 1 mm (Fig. 1 (b)). Moreover, circular samples with a thickness of 0.5 mm and a diameter of 20 mm (Fig. 1 (c)) were produced and used for biocompatibility assays (see paragraph 2.5).

Thickness and width measurements were conducted to address potential inhomogeneities in the samples. Measurements were performed at multiple sections of each specimen using a digital caliber, and average values were calculated for both thickness and width.

Table 1 shows the tested experimental variables used for material fabrication, including printer model, printing resolution, resin type, and sample thickness. Samples were fabricated through direct 3D printing using a Phrozen Sonic XL 4K 2022 printer (Phrozen Technology, Hsinchu, Taiwan) or the Accufab L4D printer (Shining 3D, Hangzhou, China). Printing was conducted in successive layers of 100 μm or 50 μm, with a down speed of 200 ms and a delay of 1000 ms. The first 6 layers were cured for 30 s, the height was 8 mm, and the up speed was 100 ms. Support structures, required to ensure the precise positioning of the samples on the build plate, were designed using the Uniz software (Uniz, San Diego, CA, USA). Upon completion of the printing process, the

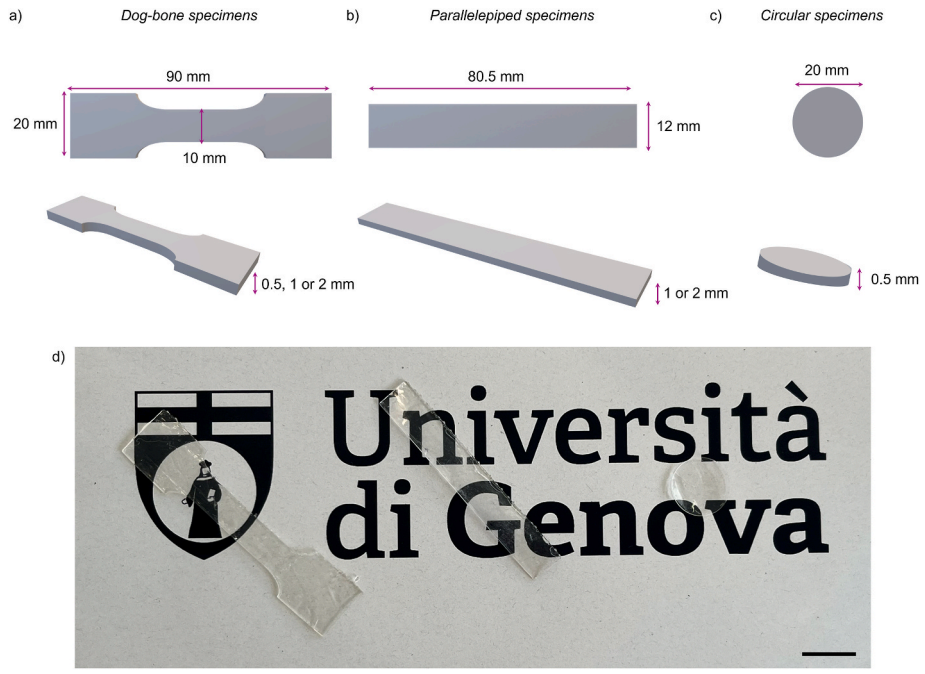

Fig. 1. Schematics and dimensions of a) dog-bone, b) parallelepiped, and c) circular test specimens. d) A photograph of samples of different shapes fabricated with the Clear A resin. Scale bar = 2 cm.

Table 1
Experimental variables tested for 3D printing, including printer model, printing resolution, resin type, and sample thickness.

Variables tested			
Printer	Phrozen Sonic XL 4K	Accufab L4D	–
Printing resolution (μm)	50	100	–
Resin	TC-85	Clear-A	–
Sample thickness (mm)[a]	0.5	1	2

[a] for tensile tests: 0.5, 1, and 2 mm; for bending tests 1 and 2 mm; for biocompatibility tests: 0.5 mm.

samples were manually detached from the build plate and the support structures were carefully removed.

2.3. Post-processing

Following printing, residual resin was removed by centrifugation at 1000 rpm for two cycles of 5 min each. Post-curing was performed under controlled conditions. In particular, samples fabricated with TC-85 resin were post-cured for 20 min using the Tera Harz Cure unit (Graphy Inc., Seoul, Korea). This compact curing system is equipped with UV LED light sources operating at a wavelength of 405 nm and delivers a UV energy density of 280,000 mJ/cm^2 within 5 min, with a UV irradiance of 1000 mW/cm^2. An integrated nitrogen generator provides an inert environment, preventing oxygen inhibition and ensuring optimal polymerization. In contrast, samples fabricated with Clear A resin were post-cured for 20 min without the use of nitrogen using the Tera Harz Cure unit.

2.4. Mechanical testing

The mechanical performance of the samples was evaluated using a Zwick/Roell Z0.5 testing machine (Zwick Roell Group, Ulm, Germany), equipped with a full-scale range of 500 N. Tensile tests were performed on the dog-bone samples at room temperature (18 °C) and continued until rupture, following the ISO 527–2:2012 standard [23]. Bending tests were conducted on the parallelepiped samples under the same environmental conditions, following an adapted version of the ISO 178:2019 standard [24]. The mechanical test parameters for tensile tests were set as follows: a preload of 1 N, with a preload speed of 1 mm/min, modulus speed of 1 mm/min, and test speed of 10 mm/min. Parameters for bending tests were 0.5 N preload, with a preload speed of 5 mm/min, and proof speed of 5 mm/min.

2.5. Biocompatibility analyses

Biocompatibility tests were essentially performed as an accomplishment of ISO-10993-5 “Biological evaluation of medical devices”, aiming to evaluate possible cytotoxic effects, due to the different components of the used materials, on cell proliferation, viability and adhesion, using two suitable cell lines. No approval from an ethics committee was required for this study, as all biological assays were performed using established commercial cell lines, in accordance with current Italian legislation and institutional policies.

2.5.1. Cell assays with human osteosarcoma cells

The test samples were prepared with the two different resins in a disk geometry with a thickness of 0.5 mm and a diameter of 20 mm with the Phrozen Sonic XL 4K printer set with a 100 μm resolution. Samples from each set were maintained in 70 % v/v Ethanol for 24 h, thoroughly washed in sterile PBS, and preserved in sterile conditions to evaluate the adhesion of human osteosarcoma cells (MG-63), a cell line already previously used to assess the suitability of orthodontic devices [21,25,26]. F12-medium and DMEM were used as growth media under standard culture conditions. The final DMEM/F12 medium (50:50) was supplemented with 2 mM L-glutamine and 10 % fetal bovine serum (FBS); medium changes were performed twice a week. To prevent cell adhesion to the well plate, the 12-well plates were pre-coated with a sterile 1 % agarose solution. To assess cell adhesion, 15,000 cells were seeded onto the material samples (one per agarose-coated well) and allowed to adhere by gravity for 48 h in 2 mL of complete medium at 37 °C under standard humidity conditions. Following incubation, samples were gently washed twice with PBS to remove non-adherent cells. The adhered cells were fixed using 4 % paraformaldehyde (PFA) for 10 min at room temperature and stained with a 1 % methylene blue solution for

5 min at room temperature. The excess stain was removed by rinsing the samples five times with PBS. Samples were then imaged using a Nikon SMZ1000 stereomicroscope (Nikon Instruments, Tokyo, Japan) equipped with a Nikon DS5 camera and accompanying imaging software.

Cell viability and metabolic activity were assessed using the Presto Blue™ assay, as already reported in the literature [27], [28]. Two different set-ups were assessed: a direct contact system and a transwell apparatus. In the former, cells seeded onto standard plastic wells were covered with the materials under testing; in the latter, materials were placed on supports equipped with perforated membranes (pores of 0.4 μm Ø), allowing them to be suspended in the culture medium without direct contact with the cells (see Fig. 5 (a) for a schematic representation). Control samples are referred to cells grown in contact with the plastic well alone. At different time points the Presto Blue dye was added at 10 % v/v to the culture medium and incubated for 4 h. Supernatant were collected, briefly decanted, and centrifuged gently (approximately 400×*g* for 5 min) to recover any cells remaining in suspension; aliquots were then analyzed spectrophotometrically using a Spectra MR multiplate reader spectrophotometer (Dynex Technologies; Chantilly, VA, USA) by measuring absorbance at 570 nm and 600 nm. Spectrophotometric analyses of Presto Blue metabolism products were performed at 0-, 2-, 4-, and 7-days post-seeding to monitor cell viability and metabolic activity over time. Results were calculated as the average of treatment replicas normalizing each 570 nm reading to its corresponding value at 600 nm, subtracting the average blank value, and normalizing the results at each time point to the initial reading at T_0, as already reported in the literature [29].

2.5.2. *Cell assays with lymphoblastoid cells*

To further assess the biocompatibility of the materials with cells devoid of attachment requirements, a human Anaplastic Large Cell Lymphoma cell line of B immortalized with the Epstein-Barr virus (designated D430B) was employed. Samples from both sets were sterilized as described earlier and utilized for cell culture experiments under direct contact or by employing a transwell set-up. D430B cells, which proliferate in suspension, do not adhere to culture plates and display a reduced cytoplasm, were previously expanded under standard culture conditions (RPMI medium supplemented with 2 mM glutamine and 10 % FBS). Experiments were conducted in 12-well plates, using 10^5 cells/well at 37 °C with standard humidity and 1 mL of medium/well. Cell viability and metabolic activity were assessed as reported in paragraph 2.5.1.

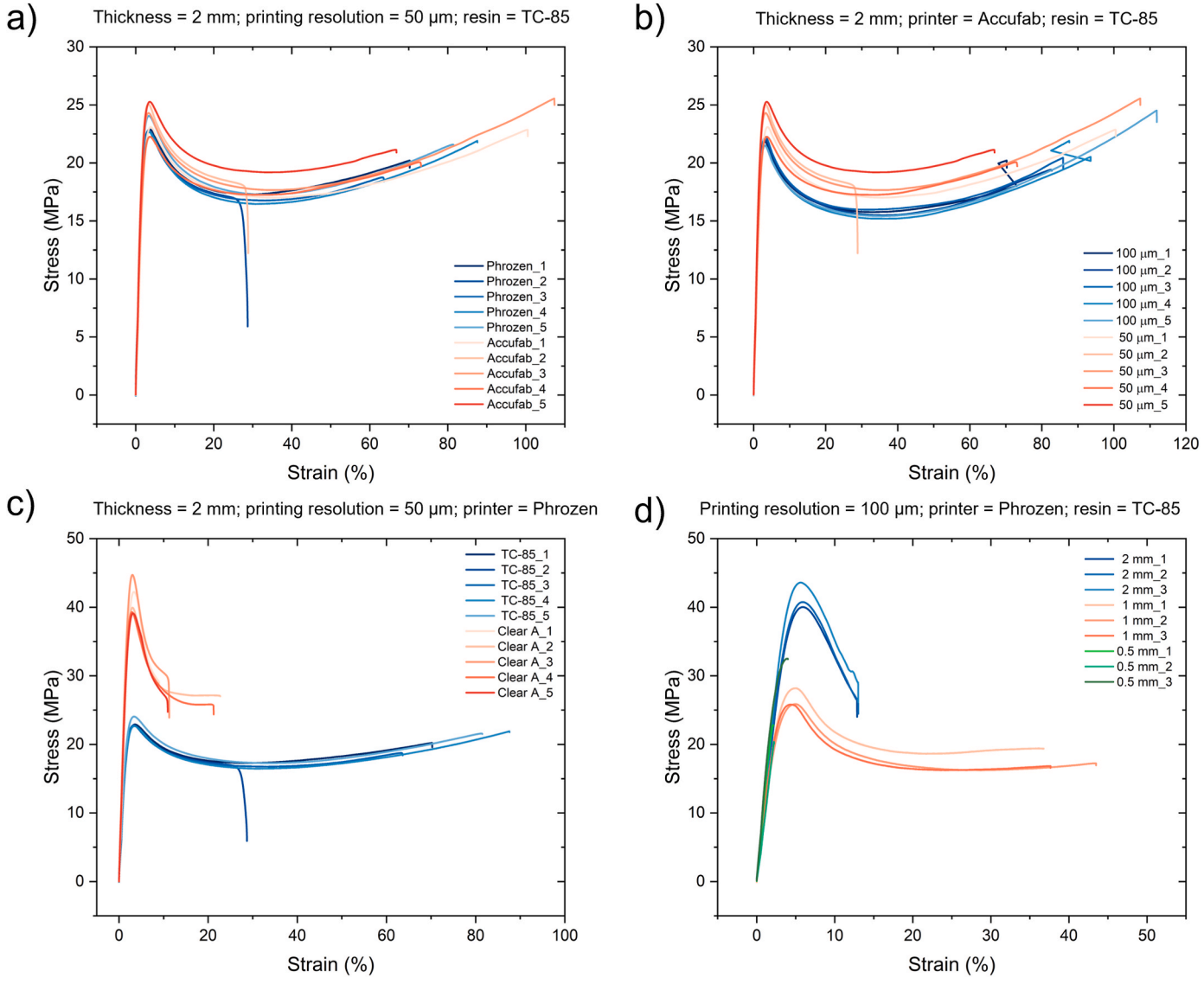

Fig. 2. Tensile stress-strain curves of samples fabricated with a) two types of printers, b) two printing resolutions, c) two types of resins, and d) three values of thickness. Five samples (n = 5) were tested for a), b), and c), and three samples (n = 3) were tested for d).

2.6. Statistical analysis

Results are expressed as the means ± S.D. of at least three independent experiments for each experimental condition. Statistical analysis was assessed using a Student's paired *t*-test using GraphPad Prism 8.0 (GraphPad Software v8.0, San Diego, CA, USA). Asterisks or other indicators (see Figure captions) indicate the following *p*-value ranges: $p > 0.05$ no symbols, * = $p < 0.05$, ** = $p < 0.01$, *** = $p < 0.001$.

3. Results

3.1. Tensile tests

The results from the tensile tests are summarized in Fig. 2 and in Tables 2 and 3. Additionally, Table 4 compares the actual measured thicknesses to evaluate the precision and consistency of the 3D printing process.

Samples printed with the Phrozen Sonic XL 4K and Accufab L4D printers showed slight differences in mechanical properties. In particular, the Phrozen printer yielded a higher tensile Young's modulus (1131.30 ± 63.99 MPa), while the Accufab printer achieved marginally better ultimate tensile strength (23.99 ± 1.16 MPa) and elongation at break (75.76 ± 27.86 %) (Fig. 2 (a) and Table 2). However, these differences were not statistically significant, which is consistent with the observation that the measured thicknesses of the samples printed by the two printers were similar (Fig. 3). This suggests that the similar dimensional accuracy achieved by both printers underpins their comparable mechanical performance.

Samples printed at a finer resolution of 50 μm demonstrated a higher ultimate tensile strength (23.99 ± 1.16 MPa, $^{**}p < 0.01$) compared to those at 100 μm (21.81 ± 0.29 MPa). However, the elongation at break was higher for samples printed at 100 μm (90.09 ± 13.05 %) compared to 50 μm (75.76 ± 27.86 %) (Fig. 2 (b) and Table 2). The observed reduction in ductility at 50 μm resolution correlates with the greater variability in measured thickness (Fig. 3), particularly in the Accufab printer, highlighting the impact of dimensional precision on mechanical properties.

Importantly, the type of resin emerged as the factor showing the most statistically significant differences between the two groups (Fig. 2 (c) and Table 2). Clear A resin demonstrated markedly superior tensile properties, with a significantly higher tensile Young's modulus (2088.28 ± 99.31 MPa, $^{***}p < 0.001$) and ultimate tensile strength (41.06 ± 2.14 MPa, $^{***}p < 0.001$). Conversely, TC-85 exhibited a much higher elongation at break (66.45 ± 20.54 %) compared to Clear A (16.48 ± 4.97 %, $^{***}p < 0.001$).

Table 2
Tensile Young's modulus, ultimate tensile strength, and elongation at break values of the tested samples fabricated with different printers, printing resolutions, and resin types.

		Tensile Young's modulus (MPa)	Ultimate tensile strength (MPa)	Elongation at break (%)
Printer	*Phrozen*	1131.30 ± 63.99	23.03 ± 0.52	66.45 ± 20.54
	Accufab	1055.95 ± 154.58	23.99 ± 1.16	75.76 ± 27.86
Printing resolution	100 μm	1051.51 ± 38.89	21.81 ± 0.29	90.09 ± 13.05
	50 μm	1055.95 ± 154.58	23.99 ± 1.16**	75.76 ± 27.86
Resin	*TC-85*	1131.30 ± 63.99	23.03 ± 0.52	66.45 ± 20.54
	Clear A	2088.28 ± 99.31***	41.06 ± 2.14***	16.48 ± 4.97***

$^{**}p < 0.01$, $^{***}p < 0.001$. The significance values reported refer to the statistical comparison between the two variables within each parametric class (tensile Young's modulus, ultimate tensile strength, and elongation at break) and among the comparison parameters (printer, printing resolution, resin).

The results displayed in Fig. 3 highlight the impact of printer type and resolution on the measured thickness of 3D-printed samples. The Phrozen printer, operating at both 100 μm and 50 μm resolutions (groups A and B, respectively), exhibited consistent thickness values indicating reliable performance. In contrast, the Accufab printer (groups C and D) demonstrated greater variability in thickness, particularly at the 50 μm resolution (group C). Statistically significant differences were observed between groups, with samples printed using the Phrozen printer at 100 μm resolution showing significantly higher thickness measurements compared to the Accufab printer ($^{***}p < 0.001$). Interestingly, increasing the resolution from 50 μm to 100 μm led to notable improvements in dimensional accuracy, although this trend was more pronounced in the Accufab printer.

Analyzing the data in Fig. 2 (d) and Table 3 reveals a strong influence of sample thickness on mechanical properties. In particular, the 2 mm samples could withstand the highest ultimate tensile strength (41.46 ± 1.89 MPa), significantly higher than the 1 mm (26.62 ± 1.36 MPa) and 0.5 mm samples (25.22 ± 6.43 MPa). Thicker samples exhibited better ductility, meaning they could endure more deformation before failure.

3.2. Bending tests

The bending test results (Fig. 4 and Table 4) demonstrate the influence of printing resolution, resin type, thickness and printer model on the mechanical properties of 3D-printed materials. A detailed analysis of the trends and specific curve features provides valuable insights into the mechanical behavior and the quality of the printing process.

During the bending tests, the material did not reach breaking point, but a maximum deflection of 7 mm was applied. Regarding printing resolution (Fig. 4 (a)), the flexural elastic modulus slightly decreases from 651.98 at 100 μm resolution to 644.31 MPa at 50 μm resolution. Similarly, the maximum flexural stress decreases from 8.80 MPa at 100 μm to 8.27 MPa at 50 μm. These differences are minimal and indicate a negligible effect of printing resolution on material properties.

In contrast, resin type has a significant impact (Fig. 4 (b)). In particular, Clear A resin shows a much higher flexural elastic modulus (1358.55 ± 177.82 MPa) and maximum flexural stress (16.44 ± 1.69 MPa) compared to TC-85 resin, which exhibits a flexural elastic modulus of 448.63 ± 59.27 MPa and maximum flexural stress of 6.11 ± 0.64 MPa. Statistical analysis indicates that these differences are highly significant ($^{***}p < 0.001$).

Surprisingly, printer models also influence the results in a statistically significant way (Fig. 4 (c)). In particular, the Accufab L4D printer yields a flexural elastic modulus of 644.31 ± 22.84 MPa and a maximum flexural stress of 8.27 ± 0.25 MPa, while the Phrozen Sonic XL 4K printer results in a modulus of 448.63 ± 59.27 MPa and stress of 6.11 ± 0.64 MPa.

Results are consistent with the conclusions reached by Zinelis et al. [18], who, in 2021, through a comparative analysis, investigated the effect of using different 3D printers on the final properties of dental aligners. The research group had indeed highlighted that the choice of different printing devices actually led to variations in the mechanical characteristics of the obtained samples in terms of Martens-Hardness, indentation-modulus, and elastic-index.

Lastly, also sample thickness plays a significant role in mechanical performance, as expected (Fig. 4 (d)). Samples with a 1 mm thickness, which exhibit a higher flexural elastic modulus (745.70 ± 22.55 MPa) and maximum flexural stress (8.40 ± 0.23 MPa), are stiffer and more resistant to bending under load compared to the 2 mm thick samples, which have a lower flexural elastic modulus (510.37 ± 42.45 MPa) and maximum flexural stress (7.13 ± 0.86 MPa). The lower stiffness and strength of the 2 mm samples suggest they are relatively more elastic and deform more readily under the same load, making them less rigid than the 1 mm samples.

Table 3
Measured thickness, tensile Young's modulus, ultimate tensile strength, and elongation at break values of the tested samples fabricated with different thickness values.

		Measured thickness (mm)	Tensile Young's modulus (MPa)	Ultimate tensile strength (MPa)	Elongation at break (%)
Sample thickness	2 mm	2.35 ± 0.08	960.45 ± 36.20	41.46 ± 1.89	12.95 ± 0.08
	1 mm	1.27 ± 0.15	907.08 ± 44.14	26.62 ± 1.36	39.22 ± 3.70
	0.5 mm	0.60 ± 0.05	1050.10 ± 252.57	25.22 ± 6.43	2.77 ± 1.05
				***$p < 0.001$ (2 mm vs 1 mm).	***$p < 0.001$ (2 mm vs 1 mm).
				*$p < 0.05$ (2 mm vs 0.5 mm).	***$p < 0.001$ (2 mm vs 0.5 mm).
					***$p < 0.001$ (0.5 mm vs 1 mm).

Table 4
Flexural elastic modulus and maximum flexural stress of 3D-printed samples under different printing resolutions, resin types, and printer models.

		Flexural elastic modulus (MPa)	Maximum flexural stress (MPa)
Printing resolution	100 μm	651.98 ± 34.10	8.80 ± 1.25
	50 μm	644.31 ± 22.84	8.27 ± 0.25
Resin	TC-85	448.63 ± 59.27	6.11 ± 0.64
	Clear A	1358.55 ± 177.82 ***	16.44 ± 1.69 ***
Printer	Phrozen	448.63 ± 59.27	6.11 ± 0.64
	Accufab	644.31 ± 22.84 ***	8.27 ± 0.25 ***
Sample thickness	2 mm	510.37 ± 42.45	7.13 ± 0.86
	1 mm	745.70 ± 22.55 ***	8.40 ± 0.23 *

*$p < 0.05$, ***$p < 0.001$. The significance values reported refer to the statistical comparison between the two variables within each parametric class (flexural elastic modulus and maximum flexural stress) and among the comparison parameters (printer, printing resolution, resin, and sample thickness).

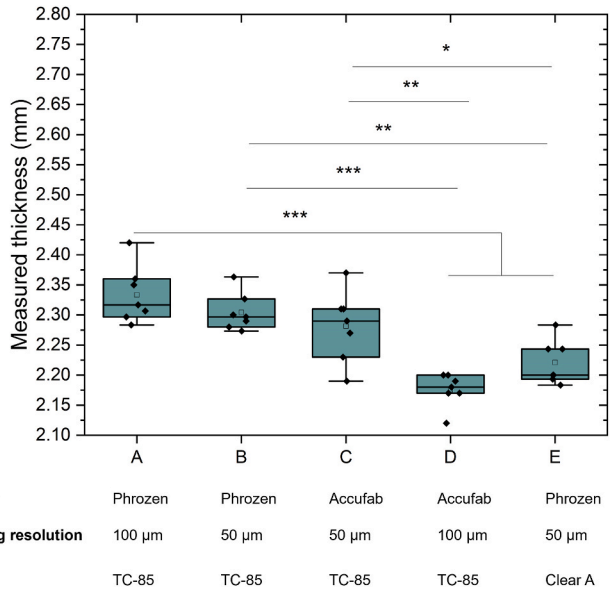

Fig. 3. Measured thickness (mm) of 3D-printed samples using different printer types (Phrozen and Accufab), resins (TC-85 and Clear A) and printing resolutions (100 μm and 50 μm). The box plots illustrate the distribution of measured values for each condition, with statistical significance indicated by * ($p < 0.05$), ** ($p < 0.01$), and *** ($p < 0.001$).

3.3. Cell adhesion and proliferation

The results from both direct contact tests and the transwell systems (Fig. 5 (a)) provide a comprehensive evaluation of the materials' effects on cell viability and metabolic activity, highlighting the impact of both direct and indirect interactions between the cells and the tested materials.

In the cell adhesion experiments using MG-63 osteoblast-like cells, neither material supported cell attachment. Instead, a few cell aggregates were observed, as happens when cells cannot find a suitable substrate for adhesion. In some instances, these aggregates remained on the material surfaces, as indicated by the red arrows in Fig. 5 (b). Additionally, cultures of MG-63 cells were maintained in contact with the materials to assess cell proliferation and viability via the Presto Blue assay. After 4 and 7 days, no significant differences in cell proliferation or viability were observed between the two materials, as shown in Fig. 5 (c). However, both materials exhibited a similarly reduced cell growth compared to the control, where cells adhered to plastic alone.

Fig. 5 (d) shows the proliferation rate of MG-63 cells cultured in transwell systems with TC-85 and Clear A resins over seven days, compared to a control. Over time, the controls showed a steady growth reaching a 3.21-fold increase in cell number by day 7; similarly, Clear-A demonstrated consistent cell growth, achieving a comparable 3.13-fold increase by the same time-point. TC-85, instead, exhibited a reduced proliferation, reaching only a 2.74 fold-increase in cell number at day 7.

The proliferation analysis of D430B cells on the two resins, TC-85 and Clear A, reveals slightly distinct behaviors (Fig. 5 (e)). In the first 48 h, cells grown on Clear A exhibit a faster initial proliferation (similar to the behavior on MG-63 (Fig. 5 (c)), increasing to approximately 1.3-fold, while cells on TC-85 resin show a slightly slower rate, reaching approximately 1.2-fold. However, after day 2, the proliferation on Clear A samples appears to plateau at around 1.5-fold the initial cell number. In contrast, cells on TC-85 exhibit a more consistent and sustained growth, reaching approximately 1.5-fold by day 4 and 1.7-fold by day 7 without, however, having a statistically significant difference after 7 days of culture (Fig. 5 (e)).

In the Transwell setup (Fig. 5 (f)), where cells are cultured indirectly with the materials, a similar trend is observed. Initially, Clear A supports slightly faster cell proliferation (1.8-fold by day 2 vs. 1.6-fold on TC-85). However, cells grown with the two different materials reach a plateau by day 4 (Clear A: approximately 1.9-fold; TC-85 approximately 2.1-fold by day 4 and approximately 2.2-fold by day 7).

4. Discussion

The results obtained from both mechanical testing and biocompatibility assessments highlight the important relationship between 3D printing settings and the properties of polymeric materials used in the production of orthodontic aligners. From the tensile tests, the comparison of 3D printing processes revealed that both the two printing resolutions and the two printers provided similar performance, with no statistically significant differences in mechanical properties. On the other hand, the type of resin used showed the most pronounced differences in tensile and bending properties. The differences were significant for all parameters considered. These mechanical differences are likely to impact the accuracy and clinical performance of the orthodontic aligners. It is reasonable to assume that a material with higher tensile strength better withstands large forces, which helps ensure a more precise fit and effective force delivery to teeth. Conversely, insufficient mechanical performance may lead to deformation or premature wear, reducing the aligner's dimensional stability and, consequently, the accuracy of tooth movement [30]. By observing Fig. 2 and the respective values in Tables 2 and 3 it is possible to compare the tensile mechanical properties of TC-85 and Clear-A resins at the same printing resolution (50 μm). The former has a stress-strain curve typical of a ductile material

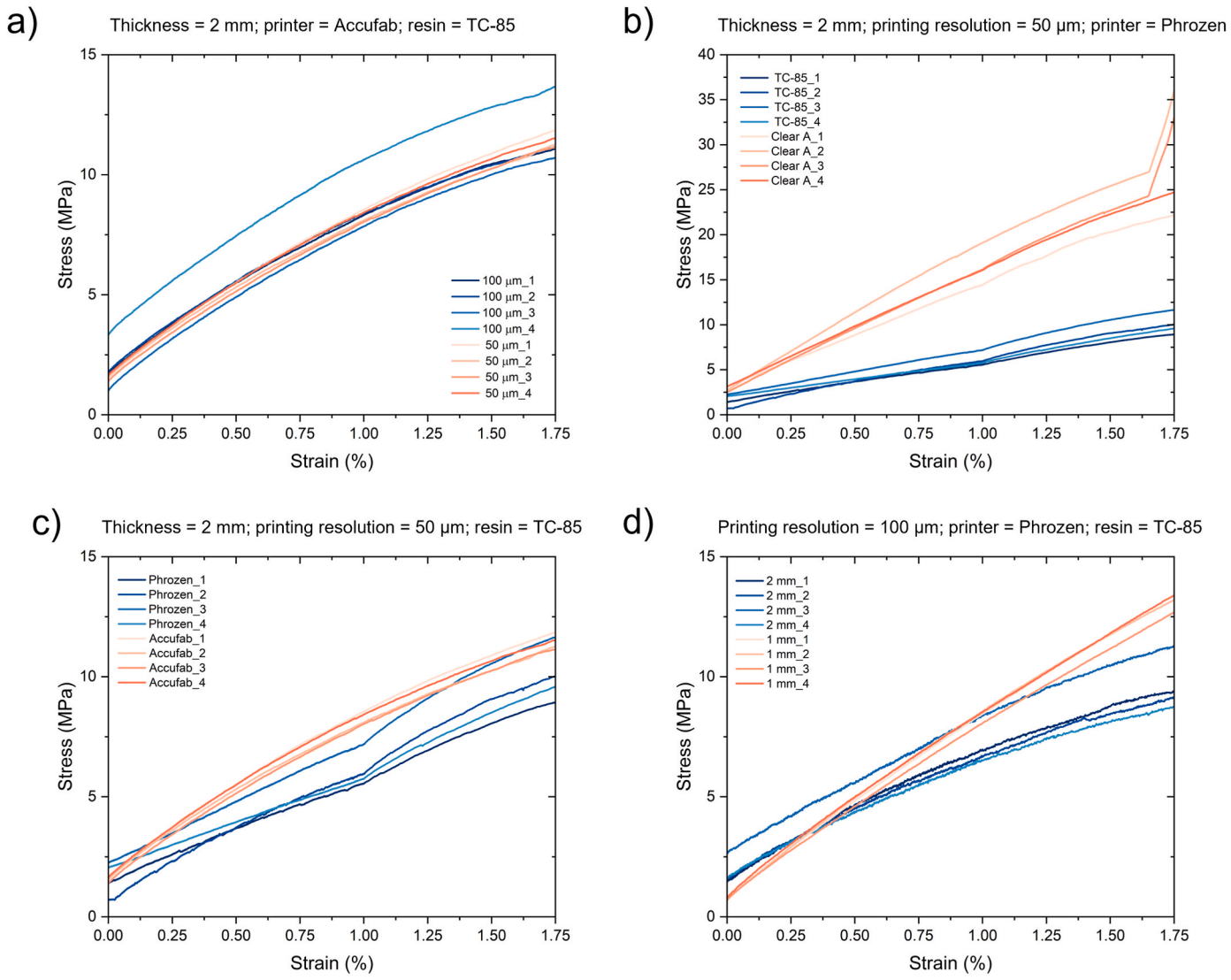

Fig. 4. Bending stress-strain curves of samples fabricated with a) two printing resolutions, b) two types of resins, c) two types of printers, and d) two values of thickness. Four samples (n = 4) for each type were tested.

and exhibits a S behavior that allows the resin to recover its original form after deformation, enhancing its adaptability. Clear A, on the other hand, has a higher elastic modulus, higher ultimate tensile strength, and a very reduced plastic plateau, at the end of which the fracture strain is only 16 %. Clear A resin's superior stiffness and strength make it suitable for aligners requiring rigidity and durability. In contrast, the higher ductility and shape memory properties of TC-85 resin suggest its potential for applications prioritizing flexibility and adaptability, which could enhance patient comfort and improve performance in scenarios involving complex dental geometries [8].

Sample thickness also played a critical role in determining mechanical properties. Thicker manufacts (2 mm) demonstrated higher strength and ductility, making them appropriate for cases requiring significant force application, such as retainers or bite planes. Thinner aligners (0.5 mm), on the other hand, exhibited greater stiffness but reduced ductility, which may improve precision in tooth movement while potentially compromising durability and adaptability [8].

From Fig. 3 it can be assessed that the choice of the Accufab printer with a layer thickness setting of 100 µm appears to be the one that minimizes oversizing of the samples, which, however remains around 10 %. Edelmann et al. [31] also investigated this aspect, demonstrating that clear aligners fabricated by 3D printing presented wall thicknesses greater than designed. Notably, the 100-µm layer height group (printed with the Accufab printer) exhibited the least average overall deviation, which not only enhances clinical and laboratory efficiency but also results in shorter print job times compared to the 50-µm layer heights [10]. It has to be noted that there is no perfect level of elasticity for dental aligners. If the material used to fabricate aligners has a very high elastic modulus (indicating significant stiffness), the aligner may become overly rigid, making it challenging for patients to insert and remove. Conversely, if the material is too flexible, it may lack the necessary stiffness to produce sufficient force for effective tooth movement [8].

The results of the bending tests confirm that while printing resolution has a minimal effect on the mechanical properties of 3D-printed materials, resin type but also printer model are critical factors influencing material performance. The statistical differences between the two printers were significant for all parameters: the samples obtained with Accufab L4D had higher values, indicating a greater stiffness of the material. Similarly to the findings of the tensile tests, significant differences also emerged from the bending tests when comparing the two resins, with relevant variations in bending elastic modulus, between the two groups. Interpreting the obtained curve, it can be concluded, in accordance with the results from the tensile tests, that the resin Clear A appears to be stiffer, hence more fragile, compared to the TC-85.

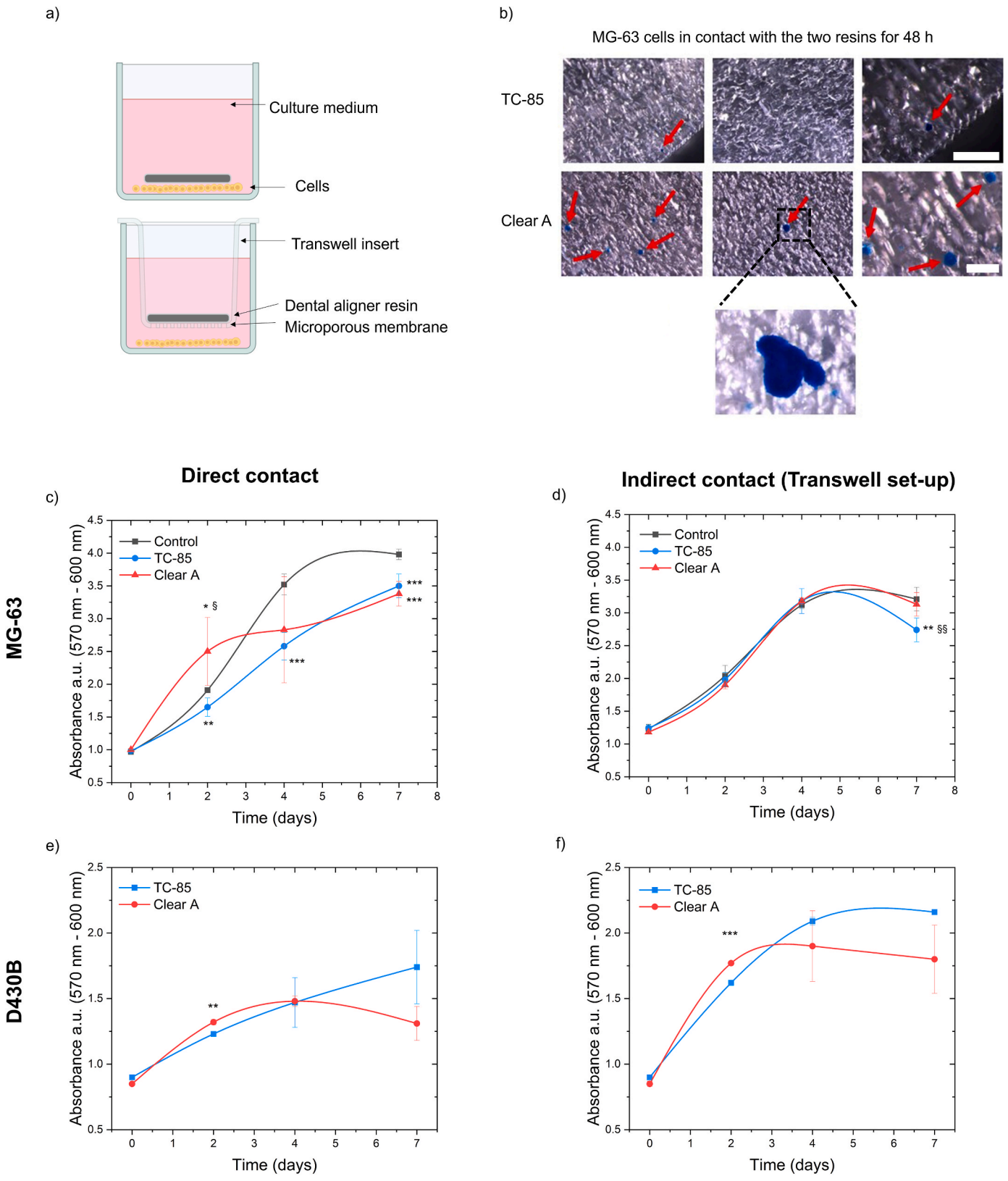

Fig. 5. Evaluation of MG-63 and D430B cell proliferation in direct and indirect contact with two resins (TC-85 and Clear A) over 7 days. (a) Schematic of the experimental setups for direct contact and indirect contact using a transwell system. (b) Optical microscopy images of MG-63 cells after 48 h of direct contact with the resins, with red arrows indicating cellular aggregates stained with methylene blue. Proliferation of MG-63 cells under direct (c) and indirect (d) contact. Proliferation of D430B cells under direct (e) and indirect (f) contact. Data points depict mean values ± SD of 5 independent determinations. Scale bar = 0.5 mm *$p < 0.05$, **$p < 0.01$, ***$p < 0.001$ (TC-85 or Clear A vs control), $^{§}p < 0.05$, $^{§§}p < 0.01$ (Clear A vs TC-85).

However, the behavior of the Clear A resin has been poorly studied in the literature, emphasizing the importance of continuing these tests, expanding the number of samples, and varying the environmental conditions.

Furthermore, sample thickness was found to significantly influence the mechanical performance. Thinner samples exhibited greater stiffness and strength, suggesting they are more rigid and less prone to deformation under load, as already pointed out from the tensile test results. In contrast, thicker samples showed more flexibility, indicating they are more elastic and can deform more readily. This highlights the importance of considering sample thickness in the design of 3D-printed components, as it plays a key role in determining material behavior under stress.

In this context, studying the effects of material aging represents a valuable direction for future research. While the resins tested in this study exhibited promising mechanical behavior, assessing how these properties evolve over time (particularly under conditions mimicking the oral environment) would further support their long-term clinical application [32]. Nonetheless, some studies suggest that mechanical properties of 3D-printed aligners are not considerably altered by intraoral aging [33,34]. Overall, these findings emphasize the importance of selecting the right combination of resin and printer model for achieving optimal material properties in 3D printing applications and underscore the need to balance mechanical performance, material properties, and patient comfort in designing dental aligners, with considerations tailored to the specific clinical requirements of each case.

As recently reported in the literature, very few studies have been conducted to study the cytotoxicity of 3D printing resins and their products [11]. Very recently, Bor et al. [35] performed XTT assays on human gingival fibroblasts (HGF) at 24, 48, and 72 h using extracts from both TC-85 and Clear A resins. Their findings, which showed minor differences among the tested resins at 48 h but comparable responses at 72 h, align with the results here presented (Fig. 5). In all cases, the materials were found to be non-cytotoxic at all time points. A similar trend was recently described by Kim et al. [36], who tested TC-85 resin extracts on L929 fibroblasts and reported that, after 24 h, cell viability remained within the thresholds of cytocompatibility as defined by ISO 10993-5. The transient decrease in cell viability observed at 24 h (Fig. 5 (c)) was also reported by other authors and it has been attributed to the initial release of water-soluble leachates, such as residual monomers, from the 3D-printed materials. Interestingly, a recovery in cell viability at later time points may reflect cellular adaptation mechanisms, such as the activation of stress-response pathways, as suggested by previous literature on similar materials [35,37]. From a practical standpoint, this issue could be mitigated by rinsing or soaking the printed devices in water prior to use, a simple yet effective strategy to reduce the initial release of leachates and improve biocompatibility. Further supporting this view, Pratsinis et al. [34] demonstrated that any substances released from TC-85 aligners aged in water for 14 days were not cytotoxic to human gingival fibroblasts, did not increase intracellular reactive oxygen species, and did not induce estrogenic activity. Overall, the results presented here indicate that both TC-85 and Clear A materials, when tested under direct and indirect contact conditions, do not exhibit cytotoxic effects that would impair cell viability or proliferation. The observed lack of cell attachment on both materials in the direct contact tests is noteworthy, as it suggests that neither material promotes favorable conditions for cell adhesion. This is particularly relevant in applications such as dental aligners, where preventing cell growth on the surface of the device can be advantageous. The inability of the cells to adhere to these surfaces may be beneficial, as it can prevent cell growth originating from minor lesions in the buccal epithelium on the mobile surfaces of the device. Indeed, the slightly reduced growth in the contact growth tests of the two resins, compared to the control group, are likely to be attributed to a mechanical rubbing effect: the physical interaction between the cells and the materials even during simple experimental procedures (*i.e.* medium change) may cause detachment of some cells, potentially affecting the proliferation evaluation. This interpretation is also in agreement with recent findings by Iodice et al. [38], who observed limited adhesion and proliferation of human fibroblasts on TC-85 resin surfaces, further supporting the notion that such materials do not favor cell attachment. This observation, along with the transwell set-up results for both cell lines used, suggests that the materials themselves do not release any cytotoxic or inhibitory substances under the conditions and timings tested. Interestingly the use of the D430B line allows to mimic a possible scenario of oral bleeding or of a ruptured vessel, where circulating white blood cells are present. For the D430B cell line the slightly different growth patterns observed are not related to the linear growth phase of the cells, but appear significant only when the same plateau level is reached, essentially at day 4 and onwards, for each contact condition. Given the assessed timings and the relative standard deviation values for those time-points, these differences can be reasonably ascribed to over-growing/crowding effects in the wells, rather than late cytotoxic events. Therefore, based on the results of both direct and indirect contact experiments, neither material appears to have any cytotoxic or cytostatic properties, and they both support cell viability, albeit at slower rates than cells grown on plastic controls.

Despite the encouraging results obtained, this study presents some limitations that should be acknowledged. All mechanical and biocompatibility assessments were conducted under controlled laboratory conditions which, although standardized and reproducible, do not fully replicate the complexity of the intraoral environment. Factors such as temperature fluctuations, enzymatic activity, continuous mechanical stress, and prolonged exposure to saliva may affect the mechanical stability of 3D-printed aligners over time [20,39,40]. Although two widely used resins and printers were selected, the results may not be fully generalizable to all materials and technologies currently available. Another limitation is the lack of surface roughness characterization, which could play a role in biological response. In addition, aging protocols were not included in the present investigation; the implementation of simulated aging conditions (such as water immersion, thermocycling, or dynamic fatigue testing) could offer further insight into the long-term performance and durability of the printed devices.

5. Conclusion

This study provides a comprehensive comparison of the mechanical and biocompatibility properties of TC-85 and Clear A resins for the fabrication of 3D-printed dental aligners under varying printing conditions. By systematically evaluating tensile strength, bending resistance, and biocompatibility through cell adhesion and proliferation assays, critical relationships were identified between printing parameters, material performance, and biological safety. Among all the factors examined, the printing resolution was found to have the least impact on the mechanical properties. In contrast, the resin type had the most substantial effect on material behavior. Significant differences in tensile modulus (1131 vs 2088 MPa for TC-85 and Clear A resins, respectively), ultimate tensile strength (23 vs 41 MPa), and elongation at break (66 % vs 16 %) were observed between the two resins tested, thereby affecting the overall mechanical behavior of the samples, with Clear A exhibiting superior stiffness and strength, making it ideal for applications requiring rigidity and durability. The TC-85 resin, on the other hand, demonstrated higher ductility coupled with a novel shape memory behavior, suggesting its suitability for applications requiring flexibility and adaptability, which could enhance patient comfort in complex dental geometries. Additionally, sample thickness was found to influence mechanical performance, with thicker samples showing higher strength and ductility, while thinner samples exhibited greater stiffness but lower ductility. These findings highlight the importance of selecting the right combination of resin and printer model, along with the appropriate sample thickness, to achieve optimal mechanical performance for specific clinical needs. In terms of biocompatibility, both resins, TC-85 and

Clear A, exhibited no cytotoxic effects when tested under both direct and indirect contact conditions, supporting cell viability and proliferation, while not releasing cytotoxic substances, further reinforcing their suitability for prolonged oral contact. This study is the first to systematically investigate the interplay of printing resolutions, sample thickness, and resin type on the functional and biological outcomes of dental aligners. By bridging the knowledge gap in resin-specific performance under varied additive manufacturing techniques, these findings offer practical insights for optimizing aligner production. Overall, the study underscores the importance of considering both mechanical properties and biocompatibility when designing 3D-printed dental devices, with particular attention to resin choice, printer settings, and sample thickness to meet the specific requirements of orthodontic treatment.

Declaration of competing interest

The authors declare that they have no known competing financial interests or personal relationships that could have appeared to influence the work reported in this paper.

References

[1] McLaughlin RP, Bennett JC. The transition from standard edgewise to preadjusted appliance systems. J Clin Orthod 1989;23:142–53.

[2] Andrews LF. The straight-wire appliance. British Journal of Orthodontics 1979;6:125–43. https://doi.org/10.1179/bjo.6.3.125. PMID: 297458.

[3] Schuster G, Reichle R, Bauer RR, Schopf PM. Allergies induced by orthodontic alloys: incidence and impact on treatment. Results of a survey in private orthodontic offices in the Federal State of Hesse, Germany. Journal of Orofacial Orthopaedics, Jan 2004;65(1):48–59. https://doi.org/10.1007/s00056-004-0312-4.

[4] Niu C, Li D, Zhang Y, Wang Y, Ning S, Zhao G, Ye Z, Kong Y, Yang D. Prospects for 3D-printing of clear aligners—a narrative review. Frontiers in Materials 2024;11.

[5] Paradowska-Stolarz A, Malysa A, Mikulewicz M. Comparison of the compression and tensile modulus of two chosen resins used in dentistry for 3D printing. Materials 2022;15. https://doi.org/10.3390/ma15248956.

[6] Paradowska-Stolarz A, Wezgowiec J, Mikulewicz M. Comparison of two chosen 3D printing resins designed for orthodontic use: an in vitro study. Materials 2023;16. https://doi.org/10.3390/ma16062237.

[7] Rajasekaran A, Chaudhari PK. Integrated manufacturing of direct 3D-printed clear aligners. Front Dent Med 2023;3.

[8] Bichu YM, Alwafi A, Liu X, Andrews J, Ludwig B, Bichu AY, Zou B. Advances in orthodontic clear aligner materials. Bioact Mater 2023;22:384–403. https://doi.org/10.1016/j.bioactmat.2022.10.006.

[9] Šimunović L, Čekalović Agović S, Marić AJ, Bačić I, Klarić E, Uribe F, Meštrović S. Color and chemical stability of 3D-printed and thermoformed polyurethane-based aligners. Polymers 2024;16. https://doi.org/10.3390/polym16081067.

[10] Favero CS, English JD, Cozad BE, Wirthlin JO, Short MM, Kasper FK. Effect of print layer height and printer type on the accuracy of 3-dimensional printed orthodontic models. Am J Orthod Dentofacial Orthop 2017;152:557–65. https://doi.org/10.1016/j.ajodo.2017.06.012.

[11] Panayi N, Cha J-Y, Kim KB. 3D printed aligners: material science, workflow and clinical applications. Semin Orthod 2023;29:25–33. https://doi.org/10.1053/j.sodo.2022.12.007.

[12] Piedra-Cascón W, Krishnamurthy VR, Att W, Revilla-León M. 3D printing parameters, supporting structures, slicing, and post-processing procedures of vat-polymerization additive manufacturing technologies: a narrative review. J Dent 2021;109:103630. https://doi.org/10.1016/j.jdent.2021.103630.

[13] Aktas B, Das R, Acikgoz A, Demircan G, Yalcin S, Aktas HG, Balak MV. DLP 3D printing of TiO2-doped Al2O3 bioceramics: manufacturing, mechanical properties, and biological evaluation. Mater Today Commun 2024;38:107872. https://doi.org/10.1016/j.mtcomm.2023.107872.

[14] Alkabbanie R, Aktas B, Demircan G, Yalcin S. Short carbon fiber-reinforced PLA composites: influence of 3D-printing parameters on the mechanical and structural properties. Iran Polym J (Engl Ed) 2024;33:1065–74. https://doi.org/10.1007/s13726-024-01315-8.

[15] Lo Giudice A, Ronsivalle V, Rustico L, Aboulazm K, Isola G, Palazzo G. Evaluation of the accuracy of orthodontic models prototyped with entry-level LCD-based 3D printers: a study using surface-based superimposition and deviation analysis. Clin Oral Invest 2022;26:303–12. https://doi.org/10.1007/s00784-021-03999-1.

[16] Tsolakis IA, Papaioannou W, Papadopoulou E, Dalampira M, Tsolakis AI. Comparison in terms of accuracy between DLP and LCD printing technology for dental model printing. Dent J 2022;10. https://doi.org/10.3390/dj10100181.

[17] Venezia P, Ronsivalle V, Rustico L, Barbato E, Leonardi R, Lo Giudice A. Accuracy of orthodontic models prototyped for clear aligners therapy: a 3D imaging analysis comparing different market segments 3D printing protocols. J Dent 2022;124:104212. https://doi.org/10.1016/j.jdent.2022.104212.

[18] Zinelis S, Panayi N, Polychronis G, Papageorgiou SN, Eliades T. Comparative analysis of mechanical properties of orthodontic aligners produced by different contemporary 3D printers, vol. 25. Orthodontics & Craniofacial Research; 2022. p. 336–41. https://doi.org/10.1111/ocr.12537.

[19] Heidt B, Rogosic R, Bonni S, Passariello-Jansen J, Dimech D, Lowdon JW, Arreguin-Campos R, Steen Redeker E, Eersels K, Diliën H, van Grinsven B, Cleij TJ. The liberalization of microfluidics: form 2 benchtop 3D printing as an affordable alternative to established manufacturing methods. Phys Status Solidi 2020;217:1900935. https://doi.org/10.1002/pssa.201900935.

[20] Milovanović A, Sedmak A, Golubović Z, Mihajlović KZ, Žurkić A, Trajković I, Milošević M. The effect of time on mechanical properties of biocompatible photopolymer resins used for fabrication of clear dental aligners. J Mech Behav Biomed Mater 2021;119:104494. https://doi.org/10.1016/j.jmbbm.2021.104494.

[21] Nemec M, Bartholomaeus HM, H Bertl M, Behm C, Ali Shokoohi-Tabrizi H, Jonke E, Andrukhov O, Rausch-Fan X. Behaviour of human oral epithelial cells grown on Invisalign® SmartTrack® material. Materials 2020;13. https://doi.org/10.3390/ma13235311.

[22] Francisco I, Paula AB, Ribeiro M, Marques F, Travassos R, Nunes C, Pereira F, Marto CM, Carrilho E, Vale F. The biological effects of 3D resins used in orthodontics: a systematic review. Bioengineering 2022;9. https://doi.org/10.3390/bioengineering9010015.

[23] Paradowska-Stolarz AM, Wieckiewicz M, Mikulewicz M, Malysa A, Dus-Ilnicka I, Seweryn P, Laskowska J, Figueiredo Pollamann MC, Adamska M, Wezgowiec J. Comparison of the tensile modulus of three 3D-printable materials used in dentistry. Dental and Medical Problems 2023;60:505–11.

[24] Šimunović L, Jurela A, Sudarević K, Bačić I, Haramina T, Meštrović S. Influence of post-processing on the degree of conversion and mechanical properties of 3D-printed polyurethane aligners. Polymers 2024;16. https://doi.org/10.3390/polym16010017.

[25] Fleischmann L, Crismani A, Falkensammer F, Bantleon H-P, Rausch-Fan X, Andrukhov O. Behavior of osteoblasts on TI surface with two different coating designed for orthodontic devices. J Mater Sci Mater Med 2015;26:10. https://doi.org/10.1007/s10856-014-5335-9.

[26] Hsu L-F, Chang B-E, Tseng K-J, Liao C-C, Tsai S-C, Hsiao H-Y, Lin S-C, Liao P-W, Chen Y-J, Jane Yao C-C. Orthodontic force regulates metalloproteinase-3 promoter in osteoblasts and transgenic mouse models. J Dent Sci 2022;17:331–7. https://doi.org/10.1016/j.jds.2021.11.015.

[27] Marrella A, Dondero A, Aiello M, Casu B, Olive D, Regis S, Bottino C, Pende D, Meazza R, Caluori G, Castriconi R, Scaglione S. Cell-laden hydrogel as a clinical-relevant 3D model for analyzing neuroblastoma growth, immunophenotype, and susceptibility to therapies. Front Immunol 2019;10.

[28] Marrella A, Tedeschi G, Giannoni P, Lagazzo A, Sbrana F, Barberis F, Quarto R, Puglisi F, Scaglione S. "Green-reduced" graphene oxide induces in vitro an enhanced biomimetic mineralization of polycaprolactone electrospun meshes. Mater Sci Eng C 2018;93:1044–53. https://doi.org/10.1016/j.msec.2018.08.052.

[29] Alfei S, Giannoni P, Signorello MG, Torazza C, Zuccari G, Athanassopoulos CM, Domenicotti C, Marengo B. The remarkable and selective in vitro cytotoxicity of synthesized bola-amphiphilic nanovesicles on etoposide-sensitive and -resistant neuroblastoma cells. Nanomaterials 2024;14. https://doi.org/10.3390/nano14181505.

[30] Li J, Si J, Xue C, Xu H. Seeking orderness out of the orderless movements: an up-to-date review of the biomechanics in clear aligners. Prog Orthod 2024;25:44. https://doi.org/10.1186/s40510-024-00543-1.

[31] Edelmann A, English JD, Chen SJ, Kasper FK. Analysis of the thickness of 3-dimensional-printed orthodontic aligners. Am J Orthod Dentofacial Orthop 2020;158:e91–8. https://doi.org/10.1016/j.ajodo.2020.07.029.

[32] Paradowska-Stolarz A, Wezgowiec J, Malysa A, Wieckiewicz M. Effects of polishing and artificial aging on mechanical properties of dental LT Clear® resin. J Funct Biomater 2023;14. https://doi.org/10.3390/jfb14060295.

[33] Can E, Panayi N, Polychronis G, Papageorgiou SN, Zinelis S, Eliades G, Eliades T. In-house 3D-printed aligners: effect of in vivo ageing on mechanical properties. EJO (Eur J Orthod) 2022;44:51–5. https://doi.org/10.1093/ejo/cjab022.

[34] Pratsinis H, Papageorgiou SN, Panayi N, Iliadi A, Eliades T, Kletsas D. Cytotoxicity and estrogenicity of a novel 3-dimensional printed orthodontic aligner. Am J Orthod Dentofacial Orthop 2022;162:e116–22. https://doi.org/10.1016/j.ajodo.2022.06.014.

[35] Bor S, Kaya Y, Demiral A, Güngörmüş M. Post-process cytotoxicity of resins in clear aligner fabrication. Polymers 2025;17. https://doi.org/10.3390/polym17131776.

[36] Kim J-E, Mangal U, Yu J-H, Kim G-T, Kim H, Seo J-Y, Cha J-Y, Lee K-J, Kwon J-S, Choi S-H. Evaluation of the effects of temperature and centrifugation time on elimination of uncured resin from 3D-printed dental aligners. Sci Rep 2024;14:15206. https://doi.org/10.1038/s41598-024-66150-6.

[37] Willi A, Patcas R, Zervou S-K, Panayi N, Schätzle M, Eliades G, Hiskia A, Eliades T. Leaching from a 3D-printed aligner resin. EJO (Eur J Orthod) 2023;45:244–9. https://doi.org/10.1093/ejo/cjac056.

[38] Iodice G, Ludwig B, Polishchuk E, Petruzzelli R, Di Cunto R, Husam S, Farella M. Effect of post-printing curing time on cytotoxicity of direct printed aligners: a pilot study. Orthod Craniofac Res 2024;27:141–6. https://doi.org/10.1111/ocr.12819.

[39] Delgado JI, Kehyaian P, Fernández-Blázquez JP. Thermoplastics for clear aligners: a review. Polymers 2025;17. https://doi.org/10.3390/polym17121681.

[40] Narongdej P, Hassanpour M, Alterman N, Rawlins-Buchanan F, Barjasteh E. Advancements in clear aligner fabrication: a comprehensive review of direct-3D printing technologies. Polymers 2024;16. https://doi.org/10.3390/polym16030371.